

Rac1b enhances cell survival through activation of the JNK2/c-JUN/Cyclin-D1 and AKT2/MCL1 pathways

Gang Li^{1,4,*}, Li Ying^{2,*}, Hong Wang¹, Si-Si Wei³, Jie Chen¹, Yi-He Chen¹, Wei-Ping Xu¹, Qi-Qiang Jie⁴, Qing Zhou¹, Yi-Gang Li¹, Yi-Dong Wei⁴ and Yue-Peng Wang¹

¹ Department of Cardiology, Affiliated Xinhua Hospital, Shanghai Jiaotong University (SJTU) School of Medicine, Shanghai, China

² Department of Neurology, Affiliated Xinhua Hospital, Shanghai Jiaotong University (SJTU) School of Medicine, Shanghai, China

³ Department of Pediatrics, Affiliated Xinhua Hospital, Shanghai Jiaotong University (SJTU) School of Medicine, Shanghai, China

⁴ Department of Cardiology, Shanghai Tenth People's Hospital, Tongji University School of Medicine, Shanghai, China

* These authors have contributed equally to this work

Correspondence to: Yue-Peng Wang, email: ypwang555@aliyun.com

Yi-Dong Wei, email: ywei@tongji.edu.cn

Yi-Gang Li, email: drliyigang@outlook.com

Keywords: Rac1b, cell proliferation, apoptosis, JNK2, AKT2

Received: October 19, 2015

Accepted: February 13, 2016

Published: February 22, 2016

ABSTRACT

Rac1b is a constitutively activated, alternatively spliced form of the small GTPase Rac1. Previous studies showed that Rac1b promotes cell proliferation and inhibits apoptosis. In the present study, we used microarray analysis to detect genes differentially expressed in HEK293T cells and SW480 human colon cancer cells stably overexpressing Rac1b. We found that the pro-proliferation genes JNK2, c-JUN and cyclin-D1 as well as anti-apoptotic AKT2 and MCL1 were all upregulated in both lines. Rac1b promoted cell proliferation and inhibited apoptosis by activating the JNK2/c-JUN/cyclin-D1 and AKT2/MCL1 pathways, respectively. Very low Rac1b levels were detected in the colonic epithelium of wild-type Sprague-Dawley rats. Knockout of the rat Rac1 gene exon-3b or knockdown of endogenous Rac1b in HT29 human colon cancer cells downregulated only the AKT2/MCL1 pathway. Our study revealed that very low levels of endogenous Rac1b inhibit apoptosis, while Rac1b upregulation both promotes cell proliferation and inhibits apoptosis. It is likely the AKT2/MCL1 pathway is more sensitive to Rac1b regulation.

INTRODUCTION

The small GTPase, Rac1, controls numerous cellular activities by cycling between an active GTP-bound form and an inactive GDP-bound form [1-3]. These processes are tightly regulated by three groups of proteins: guanine nucleotide exchange factors (GEFs), GTPase activating proteins (GAPs) and guanine nucleotide dissociation inhibitors (GDIs) [4, 5]. Activated Rac1 promotes cell cycle progression, angiogenesis, migration, transformation and cell survival [6-8]. Rac1 stimulates kinases such as p21-activated kinase (PAK), Jun NH2-terminal kinase (JNK) and p38 mitogen-activated protein kinase (MAPK) [9, 10], and the resulting signaling cascades lead to

activation of AP1 transcription factor. Rac1 also stimulates other transcription factors, including NF- κ B and serum response factor (SRF) [9-13]. Activation of these transcription factors leads to cyclin-D1 up-regulation, which promotes G1/S-phase progression.

Rac1 stimulates phosphatidylinositol-3 kinase (PI3K)-dependent activation of the AKT serine/threonine kinase, which suggests a role for Rac1 in anti-apoptotic signaling. Rac1 also stimulates the NADPH oxidase complex to generate reactive oxygen species, which up-regulates both cyclin-D1 and anti-apoptosis proteins [14-17]. Few mutations have been reported in Rac1, but Rac1 dysregulation has been associated with tumorigenesis [18-22].

Rac1b is an alternatively spliced form of Rac1, and is characterized by the insertion of an additional 19 amino acids (exon-3b) behind the intramolecular switch-II region [19, 23, 24]. This insertion induces conformational changes in switch-I and -II. Consequently, Rac1b exhibits impaired intrinsic GTPase activity, enhanced GEF-independent GDP/GTP exchange activity, and an inability to interact with Rho-GDI [25-27]. Thus, Rac1b exists in cells in a predominantly active GTP-bound form and triggers different downstream signaling cascades as compared to Rac1 [26-28]. Although it is reportedly transcribed in normal tissues, such as neurons, colon mucosa epithelial cells, thyroid and pancreatic ductal structures [23, 24], only low levels of Rac1b protein were detected in normal tissues adjacent to tumors of the thyroid [29] or lung [30], and in normal brain cortex in patients without cognitive impairment [31]. In contrast, Rac1b is upregulated in various malignant tumors including colorectal [24, 32-34], breast [19], lung [30, 35], thyroid [29] and pancreas [36, 37], and in Alzheimer's disease [31]. Rac1b upregulation is correlated with enhanced progression and poor prognosis [38, 39].

Rac1b promotes cell cycle progression and inhibits cell apoptosis, both of which are closely related to cell survival and tumorigenesis [33, 34, 40-42]. However, the underlying mechanisms of Rac1b in these processes are unclear. Both Matos, *et al.* [25] and Singh, *et al.* [27] reported that JNK was not involved in Rac1b-mediated cell proliferation. Matos, *et al.* showed that transient overexpression of Rac1b promoted phosphorylation and degradation of I κ B α (an NF- κ B suppressor), which stimulated NF- κ B-mediated G1/S-phase progression and inhibition of apoptosis [25, 40]. Cichon, *et al.* also showed that Rac1b was upstream of NF- κ B [39]. However, Singh, *et al.* found that Rac1b was unable to promote transcriptional activation of NF- κ B or the subsequent up-regulation of cyclin-D1 [27]. In the Rac1b-mediated proliferative pathway, the upstream cyclin-D1 regulators remain unclear. Aside from the NF- κ B-mediated pathway [39, 40], Singh, *et al.* reported that Rac1b, similarly to Rac1, could activate AKT and NADPH oxidase [27, 43]. However, the downstream effectors involved in the Rac1b-related anti-apoptotic effect are still unknown.

In this study, we established HEK293T and human colon cancer SW480 cell lines stably overexpressing Rac1b and analyzed differentially expressed genes (DEGs) *via* microarray analysis. In both stable lines, overexpressing Rac1b activated/upregulated the JNK2/C-JUN/cyclin-D1 pathway to promote cell proliferation and the AKT2/MCL1 pathway to inhibit apoptosis. Very low Rac1b levels were detected in the colon epithelia of wild-type Sprague-Dawley (SD) rats. Knockout of the rat Rac1 gene exon-3b or knockdown of endogenous Rac1b in human colon cancer HT29 cells downregulated only the AKT2/MCL1 pathway. Our study reveals that very low levels of endogenous Rac1b inhibit apoptosis and

upregulated Rac1b both promotes cell proliferation and inhibits apoptosis.

RESULTS

Establishment of stable cell lines overexpressing Rac1 or Rac1b

Over-expression of Rac1 or Rac1b was confirmed by semi-quantitative RT-PCR. At 25 PCR cycles, LV-Rac1 cells demonstrated increased Rac1 transcript as compared with LV-puro cells. Rac1b transcript was detected in neither LV-puro nor LV-Rac1 cells, but was evident in LV-Rac1b cells (Figure 1A). Up to 30 cycles, Rac1 transcript differences narrowed between LV-puro and LV-Rac1 cells due to saturation, and a faint endogenous Rac1 transcript band was observed in Rac1b cells.

Rac1 protein was increased by 1.65(\pm 0.16)-fold in LV-Rac1 cells as compared with LV-puro cells, similar to our previous report of a 2.0-fold change using a different lentiviral system [42]. Nascent Rac1b protein was only over-expressed in LV-Rac1b cells (Figure 1B). Endogenous and exogenous Rac1 localized mainly in the nucleus and cytoplasm, while exogenous Rac1b was observed mainly in the peripheral plasma membrane and cytoplasm (Figure 1C & 1D).

Rac1b promotes cell viability and cell cycle progression during serum-starvation

To study the effects of Rac1 and Rac1b on cell survival, we cultured LV-puro, LV-Rac1, and LV-Rac1b cell lines in medium containing three different serum concentrations (10%, 1%, and 0%) for 4 days, and measured CCK-8 daily as an index of cell viability. There was no significant difference in viability among cells cultured in 10% serum (Figure 2A). In 1% serum, viability was slightly lower in all three lines. Rac1 cells showed a slightly higher but comparable viability compared to LV-puro cells. LV-Rac1b cells had the highest viability ($p < 0.05$). In 0% serum, cell viabilities were further reduced. Rac1b cells demonstrated a higher viability as compared with LV-puro cells ($p < 0.05$). There were no significant differences between LV-Rac1 and LV-puro cells, or between LV-Rac1b and LV-Rac1 cells ($p > 0.05$). These results indicated that Rac1b could enhance cell viabilities in both 1% and 0% serum conditions.

In medium containing 10% serum, all three cell lines showed similar BrdU incorporation levels. The percentages of BrdU(+) cells were 34.95 \pm 1.83% (LV-puro), 40.49 \pm 4.38% (LV-Rac1) and 40.99 \pm 3.26% (LV-Rac1b) ($p > 0.05$ between any two; Figure 2B). In 1% serum, all three cell lines showed slightly reduced but comparable BrdU incorporation levels (30.75 \pm 2.17% for

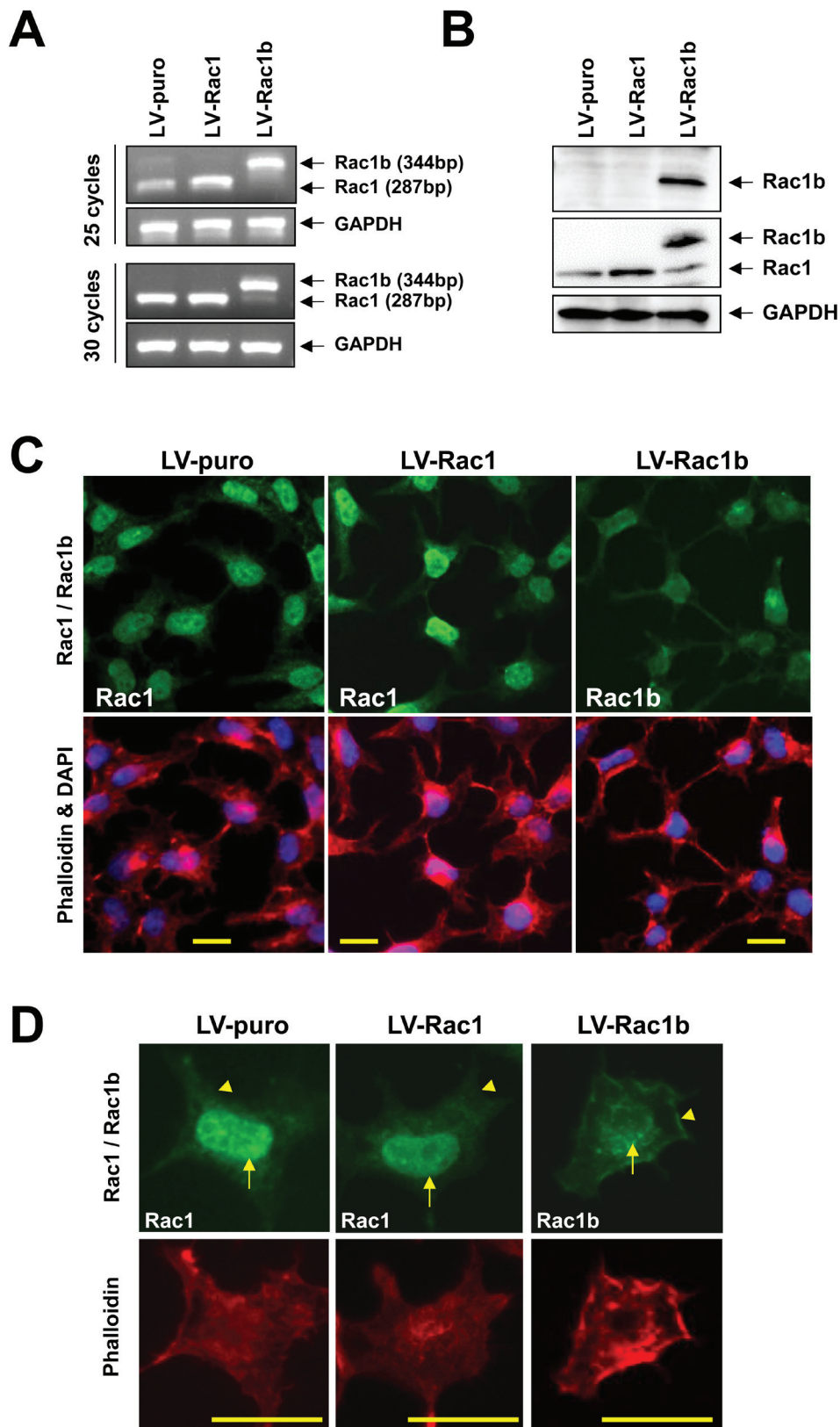


Figure 1: Stable HEK293T cell lines overexpressing Rac1 or Rac1b. **A.** Total RNA from the cell lines was reverse transcribed into cDNA, followed by PCR amplification of endogenous and/or exogenous Rac1 and Rac1b transcripts. **B.** Whole cell lysate was analyzed by western blotting using anti-Rac1b (upper), anti-Rac1 (middle), and GAPDH (lower panel) antibodies. **C.** Immunofluorescence signals of Rac1/Rac1b (upper) and phalloidin/DAPI (lower panel) confirmed 100% infection efficiency. **D.** Distribution of Rac1 and Rac1b in the nucleus (arrows) and peripheral membrane (arrow head) among the three cell lines. Bars represent 20 mm.

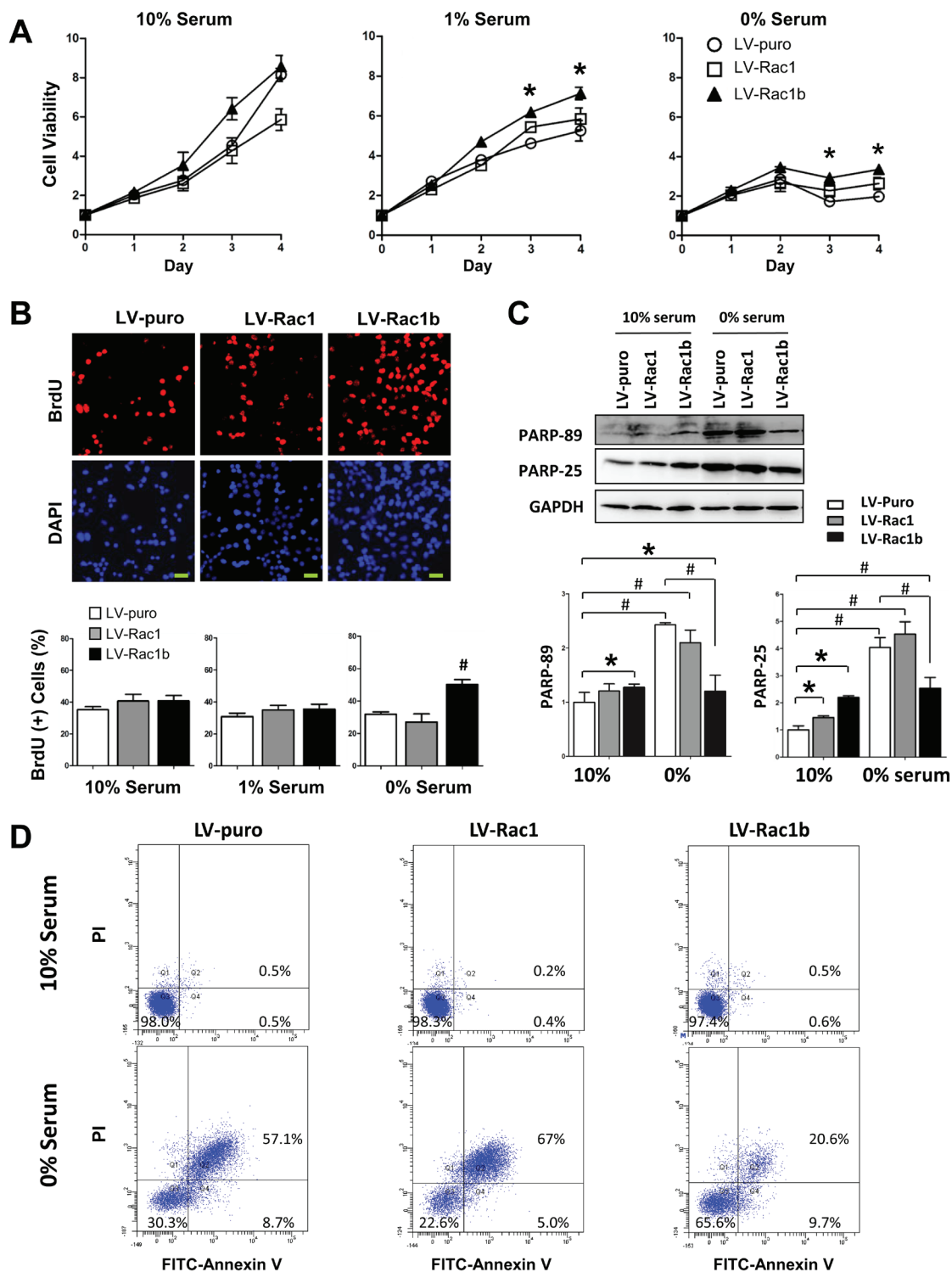


Figure 2: Rac1b promotes cell viability and cell cycle progression, and inhibits apoptosis. **A.** Cells were cultured for 0-4 days in different serum conditions as indicated and cell viabilities were assessed daily using CCK-8 assay. Results are presented as OD values normalized to day 0. * $p < 0.05$ vs. LV-puro cells. **B.** Representative images of BrdU incorporation assay for three cell lines cultured in 0% serum. Of the total DAPI-stained blue cells (lower panel), BrdU(+) cells were stained red (upper panel). Bars represent 20 mm. The percentages of BrdU(+) cells were compared in each serum condition. # $p < 0.01$ vs. LV-puro cells. **C.** Changes in cleaved PARP-89 and PARP-25 were compared in three cell-lines cultured in 10% and 0% serum. GAPDH was used as the control. Densities were first normalized to GAPDH and then to LV-puro cells in 10% serum. $N = 5$. * $p < 0.05$; # $p < 0.01$. Bars indicate comparisons. **D.** Representative results of flow cytometry in three cell lines cultured in 10% (upper) and 0% (lower panel) serum. Percentages for each cell line are labeled within each quadrant: Q-2 (late apoptosis), Q-3 (live), and Q-4 (early apoptosis).

LV-puro, 35.08±2.86% for LV-Rac1 and 35.55±3.07% for LV-Rac1b cells; $p > 0.05$ between any two). In 0% serum, as compared with LV-puro (32.66±1.38%) and Rac1 (27.21±5.04%) cells, Rac1b cells demonstrated a significantly increased percentage of BrdU(+) cells (53.74±4.42%, $p < 0.01$ for both), indicating that Rac1b could stimulate cell cycle progression under serum-starved conditions.

Rac1b inhibits apoptosis during serum-starvation

We cultured cells in medium containing 10% serum for 48 h and analyzed cleaved PARP-89 and PARP-25 levels, two well-known apoptosis markers. Compared with LV-puro cells, both cleaved PARP-89 and PARP-25 were slightly increased in LV-Rac1 cells and moderately increased in LV-Rac1b cells (Figure 2C). However, Annexin-V assays demonstrated no significant differences in the percentages of apoptotic cells (sum of quadrant-2 and -4 on flow cytometry assay) among the three cell-lines (Figure 2D). Thus, Rac1b did not inhibit apoptosis at 10% serum.

We then cultured cell lines in medium with 0% serum for 48 h. Both PARP-89 and PARP-25 were similarly increased in LV-puro and LV-Rac1 cells, but not in LV-Rac1b cells (Figure 2C). Compared with LV-puro and Rac1 cells, Rac1b cells demonstrated a significant decrease in both PARP-89 and PARP-25 ($p < 0.01$). As shown in Annexin assays (Figure 2D), LV-Rac1b cells exhibited remarkably decreased apoptosis (31.5±3.7%; $p < 0.01$) as compared with LV-puro (58.3±6.2%) and LV-Rac1 (61.0±4.8%) cells. Taken together, these results demonstrated that Rac1b effectively inhibited serum starvation-induced apoptosis.

Evidence suggests that autophagy contributes greatly to cell survival and tumorigenesis. To determine if Rac1b sustains cell survival *via* upregulation of autophagy, we analyzed LC-3-II, an indicator of autophagosome formation. Autophagy took place at a low level in 10% serum and was upregulated in 0% serum. However, there were no significant differences among the three cell lines, indicating that Rac1b-mediated cell survival was not achieved through regulation of autophagy (data not shown).

Rac1b-specific DEGs

Gene expression microarray analysis identified only 10 differentially expressed genes (DEGs) between LV-Rac1 and LV-puro cells (data not shown). In contrast, there were 482 DEGs between LV-Rac1b and LV-puro cells and 505 DEGs between LV-Rac1b and LV-Rac1 cells (Table S1). There was a high degree of overlap between the 482 and 505 DEGs (data not shown).

GO analysis of biological processes (mainly gene

function) and KEGG analysis of biological processes and signaling pathways were applied to functionally classify the 505 DEGs using the Database for Annotation, Visualization and Integrated Discovery (DAVID) [50, 51]. Of the 10 most upregulated GO Biological Process Classification cellular functions (Figure 3A), one was linked to “regulation of cell proliferation” and three were linked to “regulation of programmed cell death,” “regulation of cell death” and “regulation of apoptosis.” Of the five most significantly upregulated biological processes, regulation of cell death or apoptosis accounted for three (Figure 3B). “Pathways in cancer” and “MAPK signaling pathway” were ranked the top two most significantly upregulated pathways, while “regulation of cell proliferation” was the most significantly downregulated biological process (Figure 3C). Rac1b overexpression appeared to mainly alter cellular processes or signaling pathways related to cell proliferation and apoptosis.

We found that JNK2 (2.34-fold) and c-JUN (2.16-fold), both part of the MAPK pathway that works to promote cell cycle progression, were upregulated, but JNK1 and JNK3 were not included in the 505 DEGs (Table S1). AKT-2 (2.16-fold) and MCL1 (2.12-fold), both part of the PI3K-AKT-MCL1 pathway that regulates apoptosis inhibition, were also upregulated, but AKT-1 was not on the list of 505 DEGs. Validation qPCR results showed that JNK2 (4.0±0.31), c-JUN (4.45±0.52), AKT2 (6.13±0.37) and MCL1 (6.58±0.48 fold) were indeed upregulated in LV-Rac1b cells but not in LV-puro and LV-Rac1 cells (Figure 3D). We hypothesized that these four upregulated proteins lead to activation of two cooperative pathways and underlie the mechanisms for Rac1b-mediated cell survival.

Rac1b promotes cell cycle progression through the JNK2/c-JUN/cyclin-D1 pathway

As a known downstream effector of Rac1, JNK could phosphorylate c-JUN, which interacts with c-fos to form transcription factor AP1 and stimulates cyclin-D1 expression. Inconsistent with the qPCR results (Figure 3D), JNK2 levels were not increased in LV-Rac1b cells cultured in either the 10% or 0% serum conditions (Figure 4A & 4C). In both 10% and 0% serum, p-JNK was slightly increased in LV-Rac1 cells and significantly increased in LV-Rac1b cells compared to LV-puro cells. JNK1/2 inhibitor SP-600125 (10 mM) completely abolished both Rac1 and Rac1b-induced JNK phosphorylation.

Downstream of JNK2, we measured both expression and phosphorylation of c-JUN (p-c-JUN). In 10% serum, activated JNK2 significantly upregulated c-JUN expression in both LV-Rac1 and LV-Rac1b cells, and p-c-JUN only in LV-Rac1b cells (Figure 4A & 4C). In 0% serum, activated JNK2 upregulated c-JUN expression and phosphorylation in both cell lines. SP-600125 inhibited

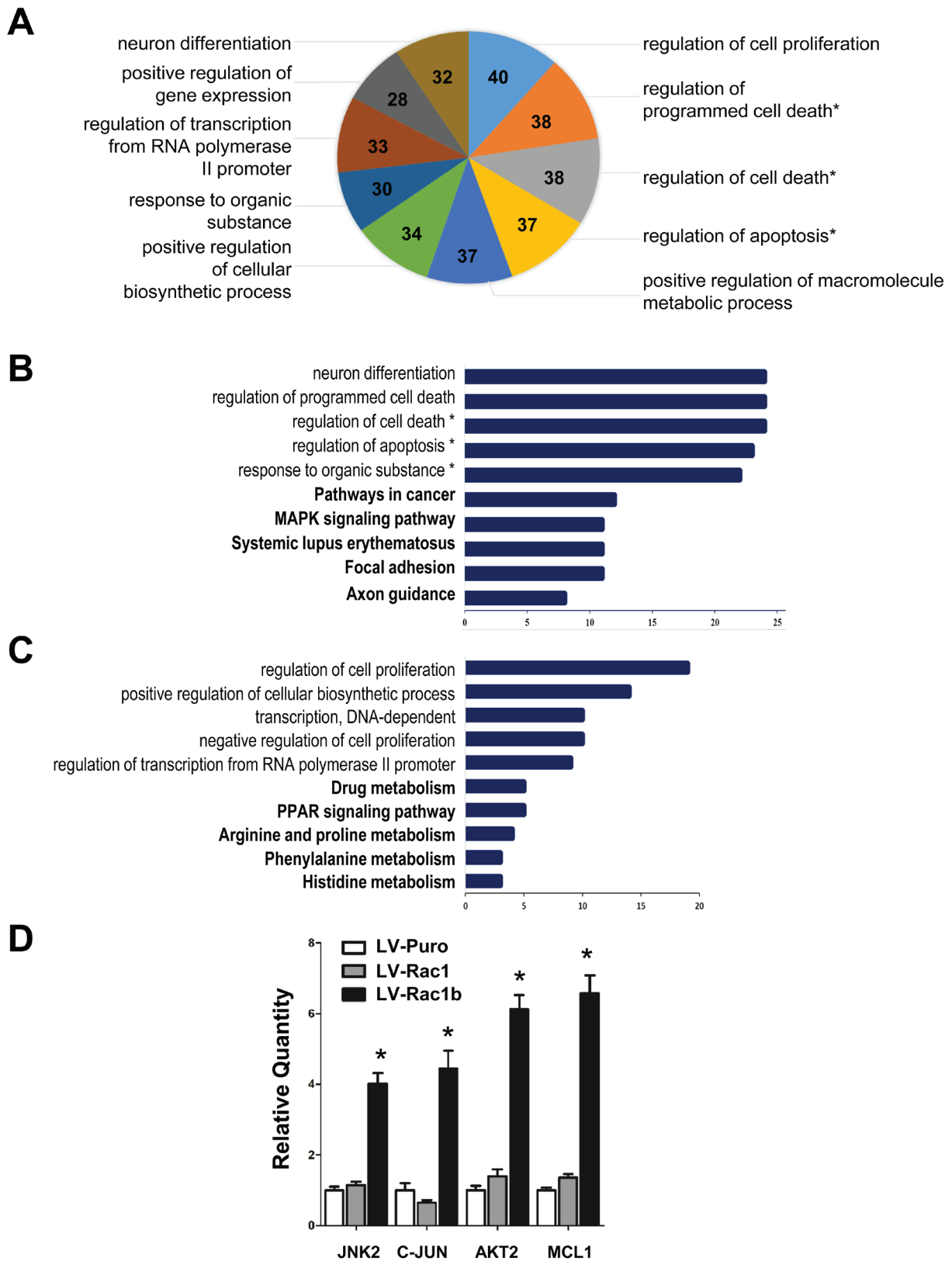


Figure 3: Rac1b-specific DEGs. In total, 505 DEGs between LV-Rac1b and LV-Rac1 cells were identified by microarray screening and were clustered based on GO analysis. **A.** A total of 347 DEGs clustered within the top 10 Rac1b-mediated biological processes or signaling pathways. The number of clustered DEGs is labeled in each section of the graph. **B.** and **C.** The top 5 biological processes and signaling pathways (bold) in which up- and down-regulated genes clustered. *related to apoptosis. **D.** Validation of JNK, c-JUN, AKT2 and MCL1 by qPCR. Data are expressed as fold change compared to controls (LV-puro cells). * $p < 0.05$ vs. LV-puro and LV-Rac1 cells.

JNK2-induced c-JUN upregulation and phosphorylation in LV-Rac1b cells.

Downstream of c-JUN, we measured expression of cyclin-D1, a key mediator of G1/S-phase progression (Figure 4A & 4C). In both 10% and 0% serum, cyclin-D1 expression was increased in LV-Rac1b cells, but not in LV-puro or LV-Rac1 cells. SP-600125 suppressed cyclin-D1 expression in LV-Rac1b cells, but not in LV-puro or LV-Rac1 cells. These results show that Rac1b upregulates JNK2/C-JUN/cyclin-D1 to promote G1/S-phase progression.

Rac1b inhibits apoptosis by upregulating the AKT2-MCL1 pathway

Previous reports showed that MCL1 is downstream of AKT and could enhance cell survival by inhibiting apoptosis [47], but whether MCL1 is involved in Rac1b-mediated anti-apoptosis is unclear. We hypothesized that Rac1b's apoptosis inhibition was AKT2-MCL1-dependent.

In 10% serum, AKT2 was increased 1.62(±0.20)-fold in LV-Rac1 cells and 1.75(±0.22)-fold in LV-Rac1b cells compared with LV-puro cells (Figure 4B & 4C). In 0% serum, AKT2 was decreased 0.76(±0.09)-fold in LV-Rac1 cells, but increased 1.30(±0.05)-fold in LV-Rac1b

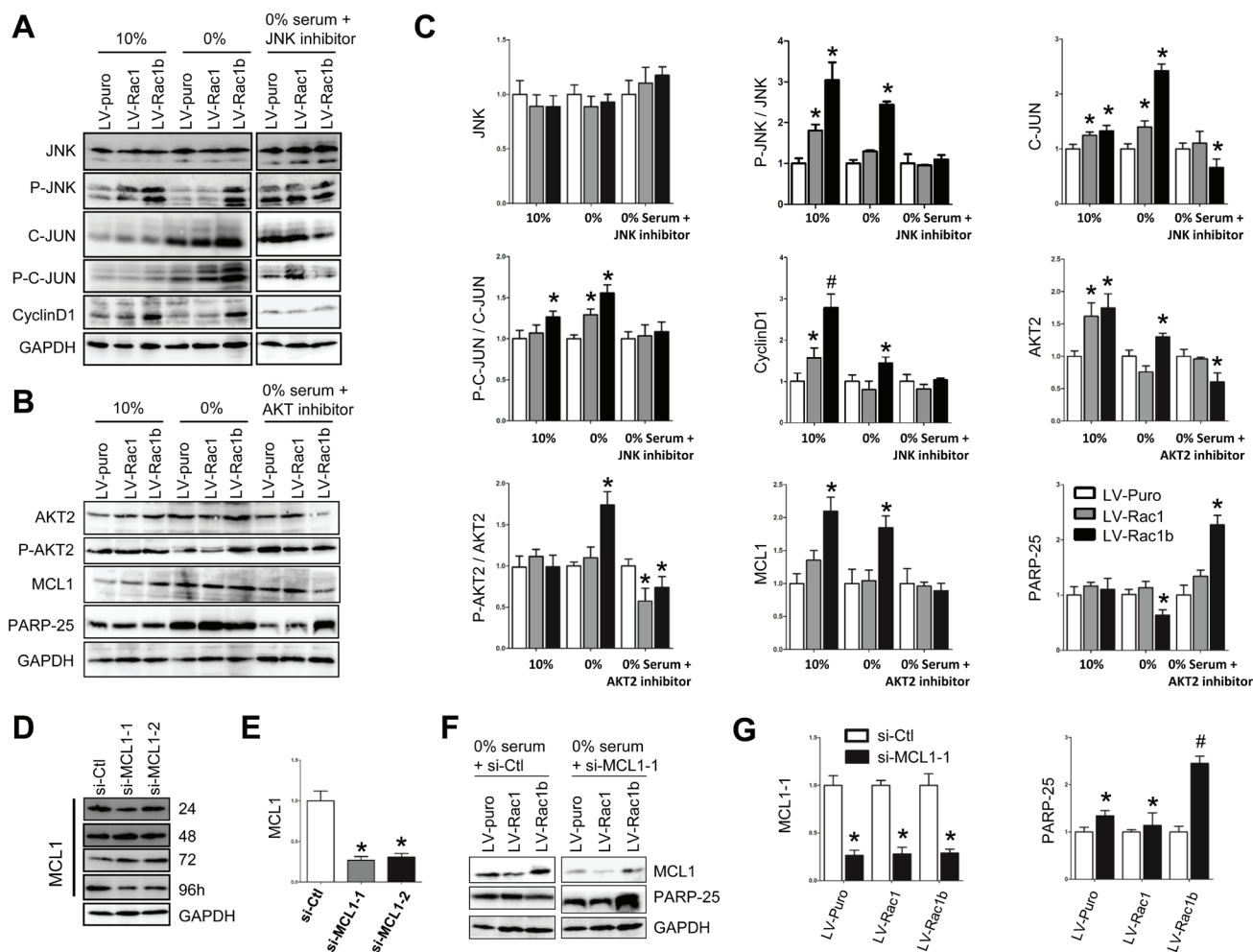


Figure 4: Rac1b promotes cell proliferation by up-regulation/activation of JNK/c-JUN/cyclin-D1 and inhibits cell apoptosis by up-regulation/activation of AKT2/MCL1. A. and B. Changes in JNK, p-JNK, c-JUN, p-c-JUN, cyclin-D1, AKT2, p-AKT, MCL1 and PARP-25 were compared by western blotting in the three cell-lines cultured in 10% and 0% serum, and 0% serum supplemented with JNK inhibitor (10 mM, 48 h; A) or AKT2 inhibitor (10 mM, 48 h; B). GAPDH was used as the control. C. Densities in A and B were first normalized to GAPDH and then to LV-puro cells in each serum condition. $N = 3\sim 5$. $*p < 0.05$ and $\#p < 0.01$ vs. LV-puro cells in each corresponding serum condition. D. Interfering effects of si-Ctl, si-MCL1-1 and si-MCL1-2 on MCL1 expression were compared 24-96 h after transfections in LV-puro cells. E. Summary of the interfering effects on MCL1 at 96 h. $N = 5$. $*p < 0.05$ vs. si-Ctl. F. Changes in MCL1 and PARP-25 were compared by western blotting in the three cell-lines after transfection of si-Ctl (left) and si-MCL1-1 (right) for 96 h. G. Densities of MCL1-1 and PARP-25 in F were first normalized to GAPDH and then to the cell-lines transfected with si-Ctl. $N = 4$. $*p < 0.05$ and $\#p < 0.01$ vs. si-Ctl.

cells. In 0% serum, CCT128930 (10 mM), a specific AKT2 inhibitor, significantly reduced AKT2 levels in LV-Rac1b cells, but not in LV-Rac1 cells.

p-AKT2 levels were not different among the three cell-lines in 10% serum (Figure 4B & 4C). In 0% serum, p-AKT2 was slightly elevated in LV-Rac1 cells, significantly elevated in LV-Rac1b cells, and was suppressed by CCT128930 in both cell lines.

In 10% serum, MCL1 was slightly upregulated in LV-Rac1 cells and significantly upregulated in LV-Rac1b cells compared with LV-puro cells (Figure 4B & 4C). In 0% serum, MCL1 was unchanged in LV-Rac1 cells but increased by 1.85(±0.17)-fold in LV-Rac1b cells. The increase in LV-Rac1b was completely abolished by CCT128930. As reflected by PARP-25 levels, CCT128930 promoted apoptosis in LV-Rac1b cells, but not in LV-Rac1 cells.

We then attenuated MCL1 expression using si-RNAs. Compared with scramble siRNA (si-Ctl), si-

MCL1-1 reduced MCL1 expression most efficiently 96 h after transfection (27%±4%), while si-MCL1-2 was less potent (35%±4%) (Figure 4D & 4E). We transfected the three cell lines with si-Ctl and si-MCL1-1 and cultured them in 0% serum for 96 h. Apoptosis was increased in LV-Rac1b cells as compared with both LV-puro and LV-Rac1 cells (Figure 4F & 4G). These results indicated that suppression of downstream MCL1 could reverse Rac1b-mediated inhibition of apoptosis.

Rac1b upregulates the JNK2/C-JUN/cyclin-D1 and AKT2/MCL1 pathways in human colon cancer cell lines

We chose the SW480 and HT29 cell lines, in which endogenous Rac1b is respectively absent and present [25, 32, 33, 54, 55], to study whether Rac1b-mediated pathway modulation also occurs in human colon cancer

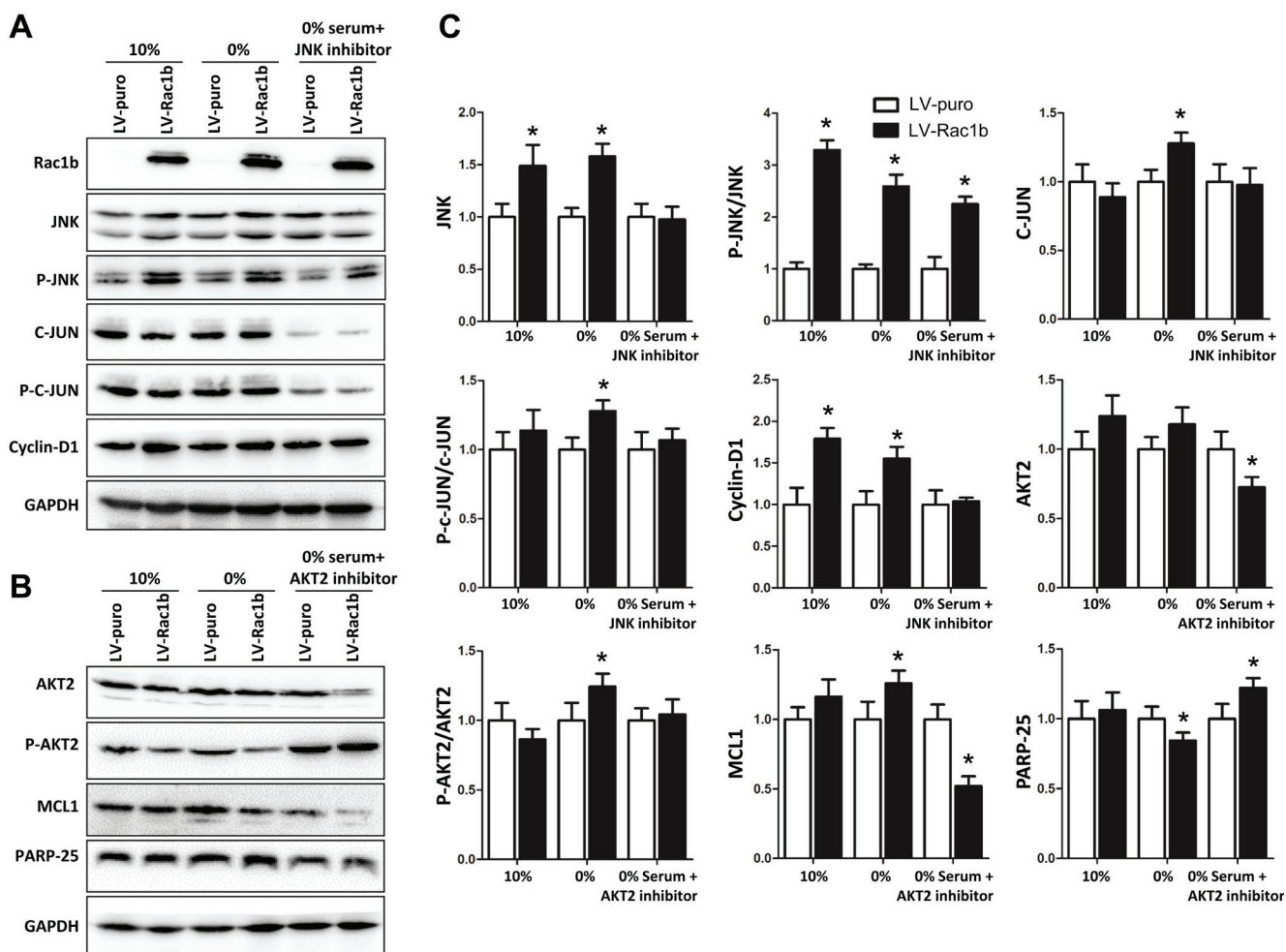


Figure 5: Rac1b upregulates and activates the JNK/c-JUN/cyclin-D1 and AKT2/MCL1 pathways in SW480 cells. Two stable SW480 cell-lines, transfected with LV-puro or LV-Rac1b, were cultured in 10% and 0% serum, and 0% serum supplemented with a JNK (10 mM, 48 h; A) or ATK2 (10 mM, 48 h; B) inhibitor. A. and B. Changes in JNK, p-JNK, c-JUN, p-c-JUN, cyclin-D1, AKT2, p-AKT, MCL1 and PARP-25 were compared by western blotting. C. Densities in A and B were first normalized to GAPDH and then to LV-puro cells. *N*= 4-5. **p* < 0.05 vs. LV-puro cells in each corresponding serum condition.

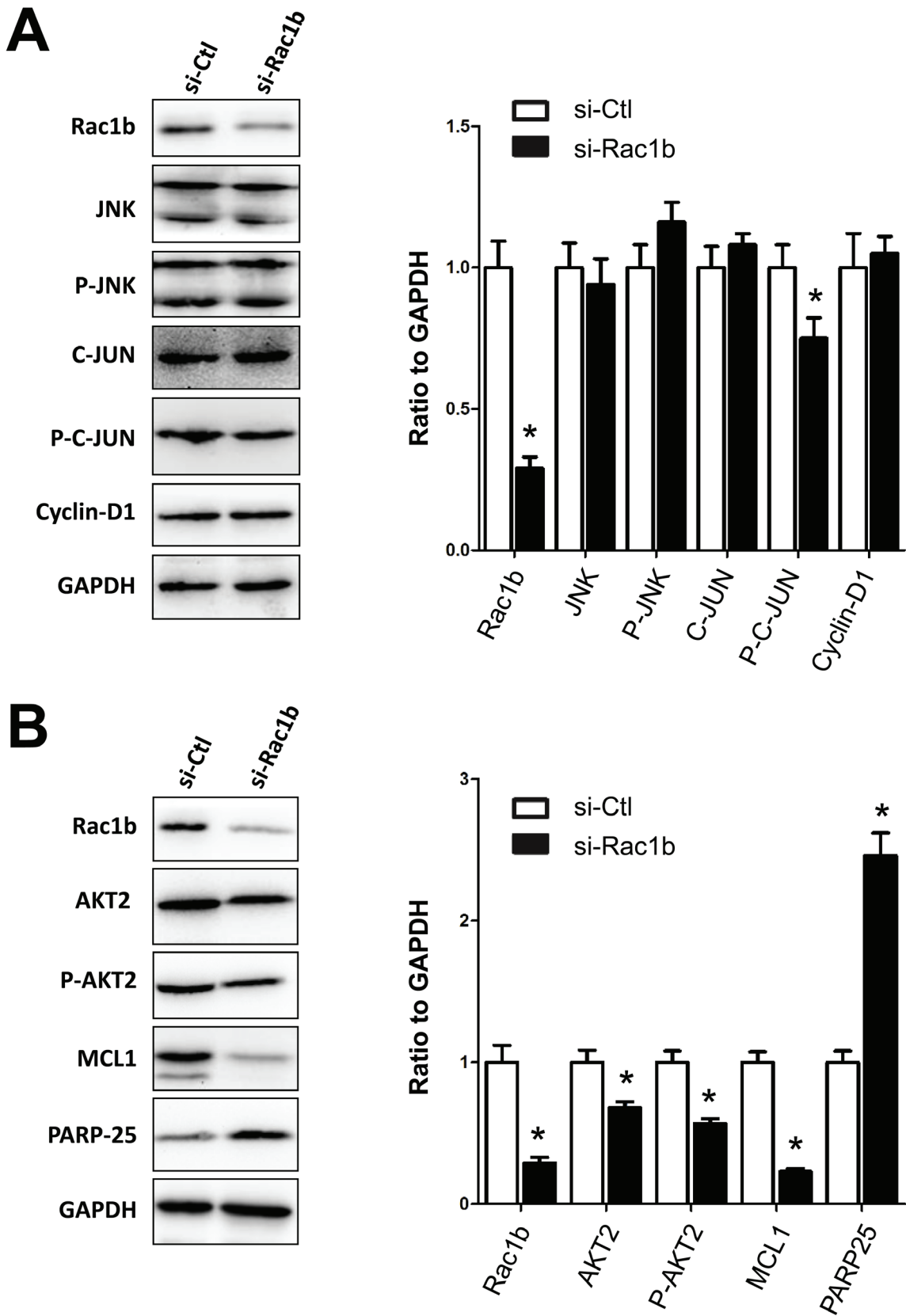


Figure 6: Rac1b upregulates and activates the AKT2-MCL1 pathway in HT29 cells. HT29 cells were transfected with scramble siRNA (si-Ctl) or siRNA specific for endogenous Rac1b for 96 h. **A.** and **B.** Changes in Rac1b, JNK, p-JNK, c-JUN, p-c-JUN, cyclin-D1, AKT2, p-AKT, MCL1 and PARP-25 were compared by western blotting. Densities were first normalized to GAPDH and then to si-Ctl. $N = 4$. * $p < 0.05$ vs. si-Ctl.

cells. We cultured SW480 cells infected with LV-puro or LV-Rac1b in 10% and 0% serum (Figure 5A & 5C). Both JNK and p-JNK were upregulated in LV-Rac1b cells in either 10% or 0% serum as compared to LV-puro cells, and this affect was blocked by SP-600125 in 0% serum. In contrast, c-JUN was unchanged in 10% serum and was slightly increased in 0% serum. Similarly, p-c-JUN was increased slightly in 0% serum, and this was inhibited by SP-600125. Cyclin-D1 increased in both 10% and 0% serum and this was inhibited by SP-600125 in 0% serum.

Although AKT2 levels were unchanged in LV-Rac1b cells in 10% and 0% serum, they were significantly reduced by the AKT2 inhibitor, CCT128930, when compared to LV-puro cells (Figure 5B & 5C). In contrast, p-AKT2 was unchanged in 10% serum, but mildly increased in 0% serum in LV-Rac1b cells. p-AKT2 was

slightly increased by the AKT2 inhibitor in LV-Rac1b cells as compared with LV-puro cells. MCL1 was unchanged in LV-Rac1b cells in 10% serum, increased in 0% serum, and significantly decreased in LV-Rac1b cells after treatment of CCT128930. Similarly, PARP-25 demonstrated no significant change in 10% serum, a mild but significant decrease in 0% serum, and a significant decrease after treatment of CCT128930. These results indicated that overexpressed Rac1b promoted cell proliferation through the JNK2/C-JUN/cyclin-D1 pathway and inhibited cell apoptosis through the AKT2/MCL1 pathway in SW480 cells.

We analyzed the JNK2/C-JUN/cyclin-D1 and AKT2/MCL1 pathways in HT29 cells with and without siRNA-knockdown of endogenous Rac1b (Figure 6A). siRNA knocked down Rac1b expression to about 29%±4%

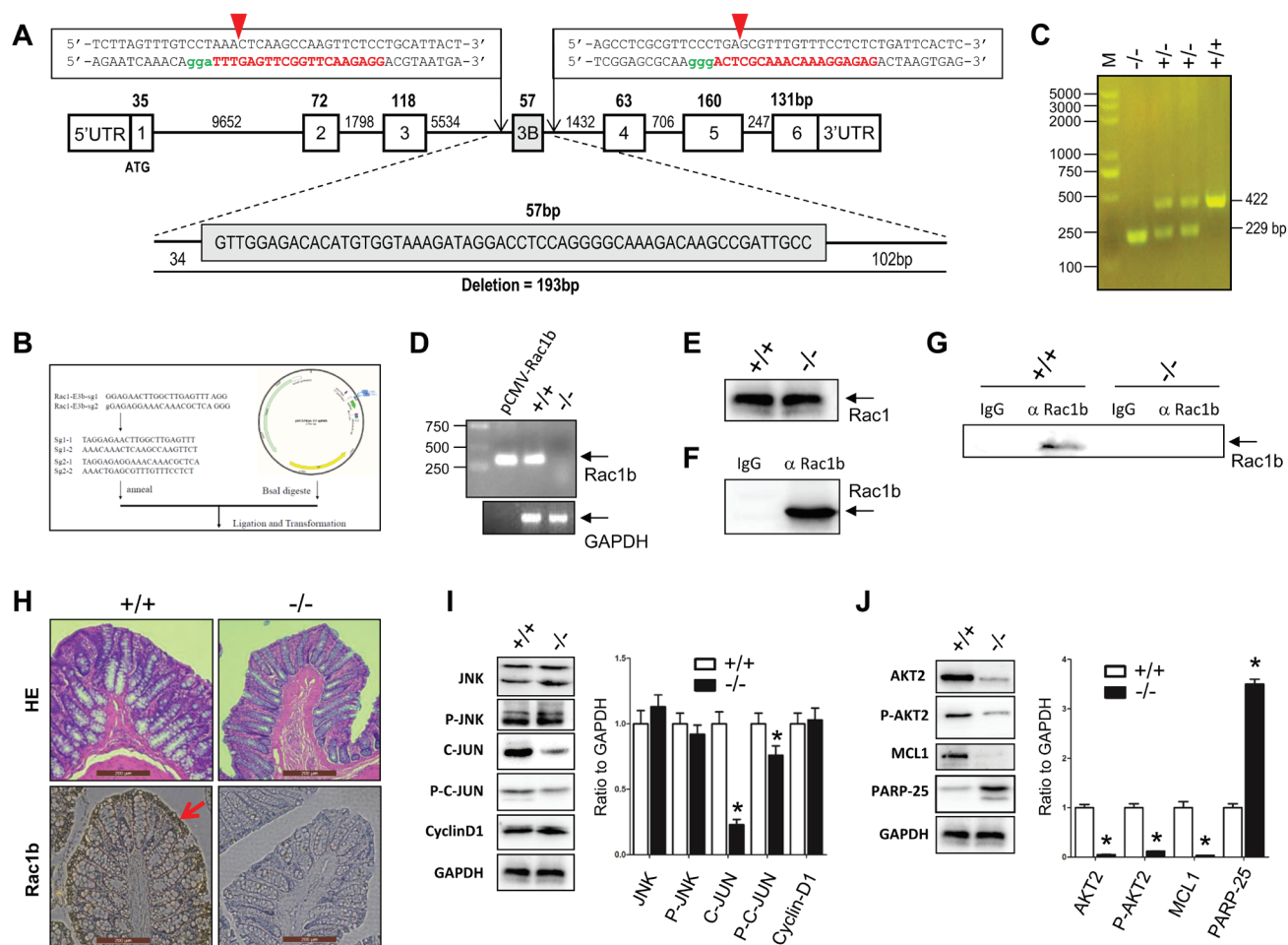


Figure 7: Generation of Rac1b^{-/-} SD rats and analysis of Rac1b-mediated AKT2/MCL1 pathway activation in the normal colon mucosa epithelia. **A.** Diagram of the rat Rac1 gene with our double Cas-9 sequences used to delete 193 bp nucleotides covering the exon-3b. The red capital letters represent recognition sequences for sgRNAs and the green letters are PAM sequences. Red arrowheads illustrate the cutting sites for CRISPR/Cas9. **B.** The sgRNA sequences and structure of pUC57Kan-T7-gRNA for transcription of sgRNA. **C.** Three genotypes of the F2 rats. **D.** and **E.** RT-PCR of Rac1b-specific transcripts (**D**) and Rac1 protein (**E**) from the colon mucosa of Rac1b^{+/+} and Rac1b^{-/-} rats. **F.** Competence of Rac1b antibodies in immunoprecipitation. **G.** Immunoprecipitation of endogenous Rac1b in the colon mucosa of rats. **H.** Immunohistochemistry of HE and Rac1b in rat colon mucosa. **I.** and **J.** The colon mucosa, harvested from WT and Rac1b^{-/-} rats, was lysed in SDS-sample buffer. Changes in JNK, p-JNK, c-JUN, p-c-JUN, cyclin-D1, AKT2, p-AKT, MCL1 and PARP-25 were compared by western blotting. Densities were first normalized to GAPDH and then to +/+. *N* = 3. **p* < 0.05 vs. Rac1b^{+/+}.

of the control level. Rac1b downregulation did not result in significant changes in JNK2, p-JNK, c-JUN, and cyclin-D levels, although p-c-JUN showed a significant decrease. However, Rac1b downregulation remarkably decreased AKT2, p-AKT2 and MCL-1 levels, and significantly increased PARP-25 (Figure 6B). These results indicated that while knockdown of endogenous Rac1b in HT29 cells did not affect the pro-proliferative JNK2/c-JUN/cyclin-D1 pathway, it dramatically attenuated the anti-apoptotic AKT2/MCL1 pathway.

Rac1b-mediation of the JNK2/C-JUN/cyclin-D1 and AKT2/MCL1 pathways in normal colon mucosa epithelia in rat

Several studies reported that normal colon mucosa epithelia have Rac1b transcripts, but no Rac1b protein [25, 32, 54, 55]. To determine whether low levels of Rac1b expression could still promote the JNK2/C-JUN/cyclin-D1 and AKT2/MCL1 pathways, we knocked out a 193bp fragment including the entire exon-3b of the Rac1 gene in SD rats using the CRISPR/Cas9 technique (Figure 7A-7C). As detected by RT-PCR using colon mucosa, the Rac1b transcript was knocked out in Rac1b^{-/-} rats (Figure 7D). In contrast, both the Rac1 transcript (data not shown) and protein (Figure 7E) were not affected in the normal colon mucosa epithelia between age- and body weight-matched WT and Rac1b^{-/-} rats.

Rac1b protein was detected only at very low levels in the normal colon mucosa epithelia of WT rats by routine western blotting. We confirmed that our Rac1b antibodies were able to immunoprecipitate our purified recombinant 6his-Rac1b (Figure 7F). We detected low levels of endogenous Rac1b protein in the normal colon mucosae of WT SD rats by immunoprecipitation, but not in Rac1b^{-/-} rats (Figure 7G). Immunohistochemical analysis showed that Rac1b was found mainly in the colon mucosa epithelia in WT rats (Figure 7H).

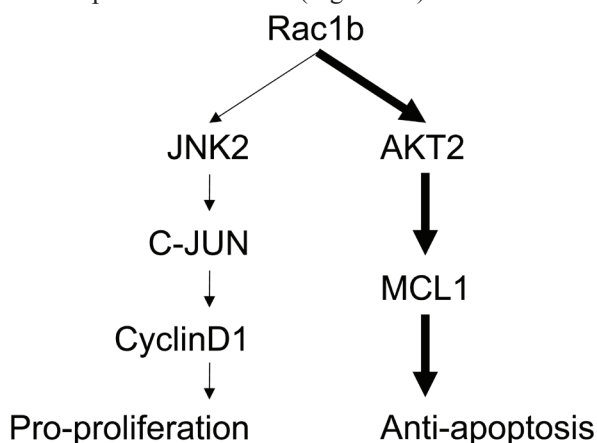


Figure 8: Schematic summary of Rac1b-mediated signaling in cell survival. Bold arrows represent the major anti-apoptotic pathway.

We found no changes in JNK2, p-JNK or cyclin-D1 in the epithelia of colon mucosa between WT and Rac1b^{-/-} rats (Figure 7I). In contrast, c-JUN and p-c-JUN decreased significantly in Rac1b^{-/-} rats. These results indicated that the JNK2/c-JUN/cyclin-D1 pathway was not changed. However, AKT2, p-AKT2 and MCL-1 were significantly decreased, and PARP-25 was increased in Rac1b^{-/-} rats (Figure 7J). Thus, knockdown of low-level Rac1b mainly promoted apoptosis through the AKT2/MCL1 pathway. Our results indicated for the first time that low levels of Rac1b are important for inhibiting apoptosis in the normal colon epithelia. Figure 8 summarizes Rac1b-mediated pro-cell cycle progression and anti-apoptosis signaling.

DISCUSSION

Rac1b is upregulated in many tumors [19, 29, 30, 33-37, 39], and we and others have reported that Rac1b enhances cell survival [33, 34, 40, 42]. However, the underlying mechanisms of this Rac1b function have not been fully elucidated. In this study, we made stable cell lines overexpressing Rac1b, confirmed Rac1b pro-proliferative and anti-apoptotic effects and identified Rac1b-specific DEGs. We found that: 1) Rac1b mainly regulates genes involved in cell proliferation and apoptosis; 2) Rac1b promotes cell cycle progression by activating JNK2, which subsequently stimulates c-JUN and up-regulates cyclin-D1; 3) Rac1b inhibits apoptosis by upregulating and activating the AKT2/MCL1 pathway; and 4) Rac1b expression level determines its impact on specific downstream pathways. At high levels, Rac1b stimulates both pro-proliferation and anti-apoptosis pathways. At low levels, it appears to only activate anti-apoptosis pathways.

Our microarray results demonstrate that there are only 10 DEGs between LV-Rac1 and LV-puro; much less than the 482 DEGs between LV-Rac1b and LV-puro and the 505 between LV-Rac1b and LV-Rac1. This may be explained by two mechanisms. First, as an important housekeeping gene, endogenous Rac1 is already redundant inside cells. Overexpression increased Rac1 levels by only about 1.6- to 2.0-fold above the basal level, both in this study (Figure 1B) and in our previous study using a different lentiviral system [42], and this is consistent with previous plasmid-mediated transient expression studies [26, 56]. Second, unlike constitutively-active Rac1b, Rac1 exists predominantly in a GDP-bound inactive form at resting state and its activation is tightly controlled. Thus, even with a 1.6- to 2.0-fold increase, Rac1 function may not be upregulated enough to result in observable and significant downstream effects as compared to controls.

Previous studies found that Rac1b activates cyclin-D1 transcription *via* NF-κB [32-34, 40] by inducing phosphorylation of the NF-κB inhibitor, IκB. However, Singh, *et al.* did not identify the role of NF-κB in the process [27]. Additionally, studies by Matos,

et al. [25] and Singh, *et al.* [27] reported that Rac1b did not activate JNK and MAPK. Therefore, the upstream regulators of cyclin-D1 in this process were still unknown. Our microarray results revealed that Rac1b could significantly enhance transcription of JNK2 and c-JUN, both of which are part of the MAPK cascade and promote cell proliferation. However, Rac1b did not upregulate JNK2 protein. Further studies are needed to investigate whether Rac1b regulates JNK2 post-transcriptionally through an unknown feedback mechanism. Rac1b significantly enhanced JNK2 phosphorylation, which then activated downstream effector c-JUN. Rac1b not only activates c-JUN but also enhances c-JUN expression and subsequently upregulates cyclin-D1 expression. That JNK inhibition by SP-600125 attenuated cyclin-D1 expression in LV-Rac1b cells further suggests that Rac1b-mediated cyclin-D1 upregulation is mainly JNK2-dependent, but not c-JUN-dependent. Our results indicate that Rac1b-mediated JNK2-dependent cyclin-D1 upregulation governs the Rac1b pro-proliferative effect.

One possible explanation for the discrepancy between our result and those of previous reports is that both Matos and Singh over-expressed JNK1 [27, 57], but not JNK2. We found that only JNK2, but not JNK1 or JNK3, was a DEG in this study. Additionally, in the previous studies, Rac1b was overexpressed transiently by transfection of a plasmid, and overexpression was sustained for only a short period of time. The current study employed stable cell lines in which sustained Rac1b overexpression was comparable to Rac1b upregulation in tumor tissues, and was therefore better suited for evaluation of cellular functions.

Previous studies identified the role of activated AKT in Rac1b-mediated cell survival [27]. We found that AKT2, but not AKT1, plays a role in Rac1b-mediated inhibition of apoptosis. p-AKT2 levels in LV-Rac1b cells were higher than in LV-Rac1 cells. We speculated that Rac1 might work through AKT1 and Rac1b through AKT2. Further studies using specific phosphor-antibodies to distinguish p-AKT1 and p-AKT2 are needed to address this question. Downstream of AKT, four proteins, MDM2, Bad, Bak and Bax, are pro-apoptotic. Another three proteins, Bcl-xL, Bcl2 and MCL1 belong to the Bcl-2 family and are anti-apoptotic [44-49]. Of these seven molecules, only MCL1 was significantly upregulated in our study. MCL1, an anti-apoptotic protein highly expressed in various cancer cells, has been associated with progression in a number of malignant tumors [47]. Using an AKT2-specific inhibitor and siRNA-mediated MCL1 knockdown, we found that AKT2/MCL1 pathway activation was directly involved in Rac1b-mediated anti-apoptosis.

We also observed that Rac1b-mediated pathway activation depends on Rac1b levels. Rac1b expressed at high, lentiviral-induced levels promotes proliferation and inhibits apoptosis. These results help to explain the

functions of Rac1b upregulation in various tumors [19, 29, 30, 32-39, 43], along with why Rac1b levels increase proportionally with enhanced malignancy [38, 39]. At low levels, Rac1b only activates the AKT2/MCL1 pathway and inhibits apoptosis. It is likely that the AKT2/MCL1 pathway is more sensitive to Rac1b regulation.

So far, several studies have detected Rac1b transcription in normal tissues, including colon mucosa epithelia, colon crypt epithelial cells, thyroid tissue, and pancreatic ductal structures [23, 24]. However, very low levels of Rac1b protein have only been detected in normal tissues adjacent to tumors [29-31]. Based on our immunoprecipitation results in rat cells, Rac1b expressed at even very low levels in normal colon mucosa epithelia is capable of moderating the AKT2/MCL1 pathway. We postulated that a low level of Rac1b exerts important function in normal cells, tissues or organs, due to Rac1b's constitutive activity and resistance to degradation [58]. However, the functional consequences of knocking out Rac1 gene exon-3b, especially changes in the incidences of tumors and inflammatory diseases, such as Crohn's disease, still need to be evaluated carefully in Rac1b^{-/-} rats.

MATERIALS AND METHODS

Antibodies and reagents

Mouse anti-Rac1 antibody was purchased from Transduction Laboratories (Lexington, KY, USA). Rabbit Rac1b antibody was generated as described previously [42]. Other rabbit antibodies were purchased from Cell Signaling (anti-LC3A/B-D3U4C, anti-JNK1/2, anti-phospho-JNK1/2, anti-c-JUN, anti-phosphor-c-JUN, anti-AKT2 and anti-MCL1; MA, USA), Biovision (anti-PARP89; Milpitas, CA, USA), Abcam (anti-PARP25, anti-cyclin-D1, anti-AKT1 and anti-phosphor-AKT2; Cambridge, MA, USA) and Proteintech (HRP-conjugated secondary antibodies; Chicago, IL, USA). SP-600125 (JNK1/2 inhibitor) and CCT128930 (AKT2 inhibitor) were purchased from Selleck Chemicals (USA).

Lentiviral construct cloning and packaging

Human Rac1 and Rac1b cDNA were cloned into the pHLV-CMVIE-Puro vector as described previously [42]. Lentivirus (Lenti-puro, Lenti-Rac1, Lenti-Rac1b) packaging and concentration were performed by co-transfecting constructs with two helper plasmids, PSPAX2 and PMD2G, in HEK293T cells with technical help from Hanheng Biotech Co., Ltd (Shanghai, China).

Cell culture, viral infection and siRNA transfection

HEK293T cells were cultured as described previously [42]. SW480 and HT-29 cells were cultured and passaged in Dulbecco's modified Eagle's medium (DMEM; HyClone, GE Healthcare Life Sci, Logan, UT, USA) supplemented with 4500mg/L high glucose, 10% fetal bovine serum, 100 units/ml penicillin, and 100 mg/ml streptomycin at 37°C and 5% CO₂. HEK293T and SW480 cells at 50-70% confluence were infected with lentivirus (Lenti-puro, Lenti-Rac1, Lenti-Rac1b) with 5 mg/ml polybrene (Sigma). Cells were selected using 2 mg/ml puromycin. For siRNA transfection, cells at 50-70% confluence were transfected with 50nM MCL1 or Rac1b siRNA (5'→3'; si-MCL1-1: AAAUAUCAACUAAGAUCUU; si-MCL1-2: AGGAAUUGAUAAUAUCUG; si-Rac1b-1: CAGUUGGAGAAACGUACGGTT; si-Rac1b-2: CGUACGGUAAGGAUAUAACCT) or scramble siRNA (AAGCGCGCUUGUAGGAUUTT; RiboBio, China) using lipofectamine-2000 (Invitrogen, USA). Interference efficiencies were checked daily for 24-96 h after transfection.

RNA isolation and quantitative real-time PCR

Total RNA isolated from the three stable cell lines using TRIzol reagent (Invitrogen, USA) was transcribed into cDNA using the 5×PrimeScript RT Kit (Takara, Japan). cDNA was measured by semi-quantitative PCR or quantitative RT-PCR (qPCR) with THUNDERBIRD SYBR qPCR Mix (Toyobo, Japan). The following primer pairs (5'→3') were used. Rac1/ Rac1b F: TGCCAATGTTATGGTAGATGG and R: TGGGAGTCAGCTTCTCTCC; JNK2

F: TACGTGGTGACACGGTACTACC and R: CACAACCTTTACCAGCTCTCC; c-JUN F: CCTTGAAAGCTCAGAACTCGGAG and R: TGCTGCGTTAGCATGAGTTGGC; AKT2 F: CATCCTCATGGAAGAGATCCGC and R: GAGGAAGAACCTGTGCTCCATG; MCL1 F: CCAAGAAAGCTGCATCGAACCAT and R: CAGCACATTCCTGATGCCACCT; and GAPDH F: TCTTACCACCATGGAGAAG and R: TGACCTTGCCACAGCCTTG.

Cell proliferation assay

Stable cell lines, seeded in 96-well plates at 3×10³ cells/well in medium containing 10% serum, were cultured overnight. Cells were then cultured in 10%, 1% or 0% serum conditions. Ten μl of Cell Counting Kit-8 (Dojindo, Japan) reagent was added to each well and

plates were incubated at 37°C for 2 h. Optical density (OD) was measured at 450nm using a microplate reader (BioTek, USA). Cell proliferation rate was calculated as: [(OD experiment - OD blank) / (OD 1st day - OD blank)] x 100%. All experiments were performed in triplicate and repeated three times [42].

BrdU incorporation assay

Cells were cultured on 10×10mm polylysine-coated cover slips, incubated with 60 μM BrdU (Sigma) for 12-16 h, fixed with cold acetone-methanol (1/1, v/v), denatured with 4M HCl, and then neutralized with 1M Tris-HCl (pH 8.0). Next, cells were incubated with mouse anti-BrdU antibodies (Sigma), Cy3-labeled secondary antibody (Jackson Laboratory, USA) and 1 μg/ml DAPI (Dojindo; Japan), and were mounted with Antifade medium (Molecular Probes, OR). BrdU(+) cells were visualized by fluorescence imaging on a Leica DMI3000B microscope [42].

Apoptosis assay

Cells cultured for 2 days in 60-mm plates in 10%, 1% or 0% serum conditions were collected and washed twice with PBS. Cells were suspended in 500 μl binding buffer, double stained with Annexin V-FITC and Propidium Iodide (KeyGEN, China) in the dark for 10 min, and analyzed by flow cytometry (BD, USA).

Microarray

Total RNA preparation from the three stable HEK293T cell lines, quality control, reverse transcription, cDNA labeling, hybridization, image acquisition, and analysis were performed by Oebiotech (Shanghai, China). Briefly, the cDNA was coupled to fluorescence dye and hybridized in four replicates to the Prime View™ Human Gene Expression Array (Affymetrix, USA). Data was normalized using the quantile algorithm by Genespring software (version 12.5; Agilent Technologies). DEGs were identified through fold changes (≥2.0 as upregulated and ≤-2.0 as down-regulated) as well as *p*-values (≤0.05), followed by GO and KEGG analysis [50, 51].

Western blotting and immunofluorescence

For western blotting, cells were rinsed with cold PBS, fixed with 10% trichloroacetic acid (Sigma) in PBS containing 2mM EDTA and 10mM dithiothreitol, washed in cold acetone containing 2mM dithiothreitol, air-dried, solubilized in SDS-sample buffer, sonicated, and subjected to SDS-PAGE. Immunofluorescence was analyzed as described previously [52, 53].

Rac1b gene knockout rat

Target sites upstream and downstream of Rac1 gene exon-3b were obtained from the rat genome using the online CRISPR design tool (<http://crispr.mit.edu>). Two oligomer pairs for the generation of sgRNA expression plasmids were annealed and cloned into the BsaI restriction site of pUC57-sgRNA (Addgene, 51132; Figure 7B). DNA was amplified for the detection of T7 promoter and sgRNA regions and the PCR products were purified before being transcribed using the MEGAshortscript Kit (Ambion, AM1354) and purified using the miRNeasy Micro Kit (Qiagen, 217084). Cas9 expression vector (Addgene, 44758) was linearized with PmeI and transcribed using the T7 Ultra Kit (Ambion, AM1345). mRNA was purified using the RNeasy Mini Kit (Qiagen, 74104) according to the manufacturer's instructions. One-cell embryos were co-injected with Cas9 and sgRNA mRNA using the FemtoJet 5247 microinjection system under standard conditions. Tail biopsies of the founder rat were collected to extract genomic DNA. Products from PCR amplification of the target region were subjected to T7 endonuclease 1 (T7EN; NEB, M0302) cleavage assay. Briefly, a 422-bp DNA fragment containing the sgRNA target site was PCR-amplified with the following primers: Rac1b-F (TATGCGACTGCAGCTTTGGA) and Rac1b-R (CTTCCGGACACCCTCCTTTC). The PCR product was purified, denatured and reannealed in NEB Buffer 2 (NEB). Hybridized PCR products were digested with T7EN for 45 min and analyzed by 2% agarose gel. The presence of mutant Rac1b alleles in tail samples was confirmed by sequencing PCR products using the primers, Rac1b-Seq-F (TGCAGCTTTGGATTCTCTG) and Rac1b-Seq-R (AAGCAGCTCGACCACTTTAC).

Immunohistology and Immunoprecipitation

The animal study was approved by the Ethics Committee of Xinhua Hospital. All animal experiments were carried out in accordance with the NIH Guide for the Care and Use of Laboratory Animals. The rats were deeply-anesthetized with pentobarbital sodium (50 mg/kg, i.p.) and whole colons were excised and divided into three segments: ascending, transverse and descending. Each segment was cut in half, weighed and rinsed in ice-cold PBS. One half of each segment was fixed in 10% formalin, embedded in paraffin, sectioned at 5 microns, and stained with hematoxylin and eosin (H&E) and Rac1b. The second half was pulverized using a tissue-tearor on ice, with 100x cocktail protease inhibitors. Smashed tissue was immediately suspended in ice-cold TLB buffer containing protease inhibitors and sonicated [52]. Supernatant was obtained by centrifugation at 14,000g for 20 min and protein concentrations were measured using the Bradford method. Supernatants underwent pre-absorptions by

protein-G beads (Roche; Indianapolis, IN, USA) for 1 h at 4°C. After removal of the beads, supernatants (1000 mg of total protein) were mixed with Rac1b antibodies (3 mg) for 4 h with rocking at 4°C. Protein-G beads were then added with an additional 4 h of rocking. Immunoprecipitates were centrifuged at 800g for 5 min at 4°C, washed four times with TLB buffer, and then resuspended in 60 ml of SDS sample buffer.

Statistics

Data are expressed as means \pm S.E. ANOVA tests and Student's *t*-tests were used to determine statistical significance. $P < 0.05$ was regarded as statistically significant.

CONFLICTS OF INTEREST

The authors declare no conflicts of interest.

GRANT SUPPORT

This work was supported by the Welcome Trust for New Principal Investigators of Xinhua Hospital (Y-P. W.), the Pujiang Project for Extraordinary Scientist of the Science and Technology Commission of Shanghai Municipality 12PJ1406400 (Y-P. W.), the Natural Science Foundation of Zhejiang Province Y2101019 (Y-P. W.), the Natural Science Foundation of China (NSFC) Grants No.81170302 (Y-P. W.), No.81270258 (Y-G. L.), No.81270193 (Y-D. W.), No.30800466 (Y-D. W.), No.81370257 (Y-P. W.), No.81470497 (J. C.) and No.81530015 (Y-G. L.).

REFERENCES

1. Burridge K, Wennerberg K. Rho and Rac take center stage. *Cell* 2004; 116: 167-179.
2. Jaffe AB, Hall A. Rho GTPases: Biochemistry and Biology. *Annu Rev Cell Dev Biol* 2005; 21: 247-269.
3. Hall A. Rho family GTPases. *Biochem Soc Trans* 2012; 40: 1378-1382.
4. Moon SY, Zheng Y. Rho GTPase-activating protein in cell regulation. *Trends Cell Biol.* 2003; 13: 13-22.
5. Heasman SJ, Ridley AJ. Mammalian Rho GTPases: new insights into their functions from *in vivo* studies. *Nat Rev.* 2008; 9: 690-701.
6. Van AL and D'Souza-Schorey C. Rho GTPases and signaling networks. *Genes Dev.* 1997; 11: 2295-2322.
7. Westwick JK, Lambert QT, Clark GJ, Symons M, Van Aelst L, Pestell RG, Der CJ. Rac regulation of transformation, gene expression, and actin organization by multiple, PAK-independent pathways. *Mol Cell Biol.* 1997; 17: 1324-1335.
8. Karlsson R, Pedersen ED, Wang Z, Brakebusch C. Rho

- GTPase function in tumorigenesis. *Biochim Biophys Acta* 2009; 1796: 91-98.
9. Minden A, Lin A, Claret FX, Abo A, Karin M. Selective activation of the JNK signaling cascade and c-Jun transcriptional activity by the small GTPases Rac and Cdc42Hs. *Cell* 1995; 81: 1147-1157.
 10. Bar SD, Hall A. Ras and Rho GTPases: a family reunion. *Cell* 2000; 103: 227-238.
 11. Hill CS, Wynne J, Treisman R. The Rho family GTPases RhoA, Rac1, and CDC42Hs regulate transcriptional activation by SRF. *Cell* 1995; 81: 1159-1170.
 12. Sulciner DJ, Irani K, Yu ZX, Ferrans VJ, Goldschmidt-Clermont P, Finkel T. Rac1 regulates a cytokine-stimulated, redox-dependent pathway necessary for NF- κ B activation. *Mol Cell Biol*. 1996; 16: 7115-7121.
 13. Archibald A, Mihai C, Macara IG, McCaffrey L. Oncogenic suppression of apoptosis uncovers a Rac1/JNK proliferation pathway activated by loss of Par3. *Oncogene* 2015; 34: 3199-3206.
 14. Keely PJ, Westwick JK, Whitehead IP, Der CJ, Parise LV. Cdc42 and rac1 induce integrin-mediated cell motility and invasiveness through PI(3)K. *Nature* 1997; 390: 632-636.
 15. Coniglio SJ, Jou TS, Symons M. Rac1 protects epithelial cells against anoikis. *J Biol Chem*. 2001; 276: 28113-28120.
 16. Wennerberg K, Ellerbroek SM, Liu RY, Karnoub AE, Burridge K, Der CJ. RhoG signals in parallel with Rac1 and Cdc42. *J Biol Chem*. 2002; 277: 47810-47817.
 17. Ueyama T, Geiszt M, Leto TL. Involvement of Rac1 in activation of multicomponent Nox1- and Nox3-based NADPH oxidases. *Mol Cell Biol*. 2006; 26: 2160-2174.
 18. Fritz G, Just I, Kaina B. Rho GTPases are over-expressed in human tumors. *Int J Cancer* 1999; 81: 682-687.
 19. Schnelzer A, Prechtel D, Knaus U, Dehne K, Gerhard M, Graeff H, Harbeck N, Schmitt M, Lengyel E. Rac1 in human breast cancer: overexpression, mutation analysis, and characterization of a new isoform, Rac1b. *Oncogene* 2000; 19: 3013-3020.
 20. Kamai T, Yamanishi T, Shirataki H, Takagi K, Asami H, Ito Y, Yoshida KI. Overexpression of RhoA, Rac1, and Cdc42 GTPases is associated with progression in testicular cancer. *Clin Cancer Res*. 2004; 10: 4799-4805.
 21. Engers R, Ziegler S, Mueller M, Walter A, Willers R, Gabbert HE. Prognostic relevance of increased Rac GTPase expression in prostate carcinomas. *Endocr Relat Cancer* 2007; 14: 245-256.
 22. Kawazu M, Ueno T, Kontani K, Ogita Y, Ando M, Fukumura K, Yamato A, Soda M, Takeuchi K, Miki Y, Yamaguchi H, Yasuda T, Naoe T, Yamashita Y, Katada T, Choi YL, Mano H. Transforming mutations of RAC guanosine triphosphatases in human cancers. *Proc Natl Acad Sci USA*. 2013; 110: 3029-3034.
 23. Jordan P, Brazao R, Boavida MG, Gespach C, Chastre E. Cloning of a novel human Rac1b splice variant with increased expression in colorectal tumors. *Oncogene* 1999; 18: 6835-6839.
 24. Matos P, Skaug J, Marques B, Beck S, Verissimo F, Gespach C, Boavida MG, Scherer SW, Jordan P. Small GTPase Rac1: structure, localization, and expression of the human gene. *Biochem Biophys Res Commun*. 2000; 277: 741-751.
 25. Matos P, Collard JG, Jordan P. Tumor-related alternatively spliced Rac1b is not regulated by Rho-GDP dissociation inhibitors and exhibits selective downstream signaling. *J Biol Chem*. 2003; 278: 50442-50448.
 26. Fiegen D, Haeusler LC, Blumenstein L, Herbrand U, Dvorsky R, Vetter IR, Ahmadian MR. Alternative splicing of Rac1 generates Rac1b, a self-activating GTPase. *J Biol Chem*. 2004; 279: 4743-4749.
 27. Singh A, Karnoub AE, Palmby TR, Lengyel E, Sondek J, Der CJ. Rac1b, a tumor associated, constitutively active Rac1 splice variant, promotes cellular transformation. *Oncogene* 2004; 23: 9369-9380.
 28. Orlichenko L, Geyer R, Yanagisawa M, Khauv D, Radisky ES, Anastasiadis PZ, Radisky DC. The 19-amino acid insertion in the tumor-associated splice isoform Rac1b confers specific binding to p120 catenin. *J. Biol. Chem*. 2010; 285: 19153-19161.
 29. Silva AL, Carmo F, Bugalho MJ. RAC1b overexpression in papillary thyroid carcinoma: a role to unravel. *Eur J Endocrinol*. 2013; 168: 795-804.
 30. Zhou C, Licciulli S, Avila JL, Cho M, Troutman S, Jiang P, Kossenkov A, Showe LC, Liu Q, Vachani A, Albelda SM, Kissil JL. The Rac1 splice form Rac1b promotes K-ras-induced lung tumorigenesis. *Oncogene* 2013; 32: 903-909.
 31. Perez SE, Getova DP, He B, Counts SE, Geula C, Desire L, Coutadeur S, Peillon H, Ginsberg SD, Mufson EJ. Rac1b increases with progressive tau pathology within cholinergic nucleus basalis neurons in Alzheimer's disease. *Am J Pathol*. 2012; 180: 526-540.
 32. Matos P, Jordan P. Rac1, but Not Rac1B, Stimulates RelB-mediated gene transcription in colorectal cancer cells. *J Biol Chem*. 2006; 281: 13724-13732.
 33. Matos P, Oliveira C, Velho S, Goncalves V, Costa LTD, Moyer MP, Seruca R, Jordan P. B-Raf V600E cooperates with alternative spliced rac1b to sustain colorectal cancer cell survival. *Gastroenterology* 2008; 135: 899-906.
 34. Matos P, Jordan P. Increased Rac1b expression sustains colorectal tumor cell survival. *Mol Cancer Res*. 2008; 6: 1178-1184.
 35. Stallings-Mann ML, Waldmann J, Zhang Y, Miller E, Gauthier ML, Visscher DW, Gregory P, Downey, Evette S, Radisky, Alan P, Fields, Derek C, Radisky. Matrix Metalloproteinase Induction of Rac1b, a Key Effector of Lung Cancer Progression. *Science Transl Med*. 2012; 4: 142ra95.
 36. Ungefroren H, Sebens S, Giehl K, Helm O, Groth S, Fandrich F, Rocken C, Sipos B, Lehnert H, Gieseler F. Rac1b negatively regulates TGF-beta1-induced cell motility

- in pancreatic ductal epithelial cells by suppressing Smad signalling. *Oncotarget* 2014; 5: 277-290. doi: 10.18632/oncotarget.1696.
37. Mehner C, Miller E, Khauv D, Nassar A, Oberg AL, Bamlet WR, Zhang L, Waldmann J, Radisky ES, Crawford HC, Radisky DC. Tumor cell-derived MMP3 orchestrates Rac1b and tissue alterations that promote pancreatic adenocarcinoma. *Mol Can Res* 2014; 12: 1430-1439.
 38. Alonso-Espinaco V, Cuatrecasas M, Alonso V, Escudero P, Marmol M, Horndler C, Ortego J, Gallego R, Codony-Servat J, Garcia-Albeniz X, Jares P, Castells A, Lozano JJ, Rosell R, Maurel J. RAC1b overexpression correlates with poor prognosis in KRAS/BRAF WT metastatic colorectal cancer patients treated with first-line FOLFOX/XELOX chemotherapy. *Eur J Cancer* 2014; 50: 1973-1981.
 39. Cichon MA, Radisky DC. ROS-induced epithelial-mesenchymal transition in mammary epithelial cells is mediated by NF- κ B-dependent activation of Snail. *Oncotarget*. 2014; 5: 2827-2838. doi: 10.18632/oncotarget.1940.
 40. Matos P, Jordan P. Expression of Rac1b stimulates NF- κ B-mediated cell survival and G1/S progression. *Exp Cell Res*. 2005; 305: 292-299.
 41. Radisky DC, Levy DD, Littlepage LE, Liu H, Nelson CM, Fata JE, Leake D, Godden EL, Albertson DG, Nieto MA, Werb Z, Bissell MJ. Rac1b and reactive oxygen species mediate MMP-3-induced EMT and genomic instability. *Nature* 2005; 436: 123-127.
 42. Ying L, Li G, Wei SS, Wang H, An P, Wang X, Guo K, Luo XJ, Zhou Q, Li W, Yu Y, Li YG, Duan JL, Wang YP. Sanguinarine inhibits Rac1b-rendered cell survival enhancement by promoting apoptosis and blocking proliferation. *Acta pharmacol Sin*. 2015; 36: 229-240.
 43. Lee K, Chen QK, Lui C, Cichon MA, Radisky DC, Nelson CM. Matrix compliance regulates Rac1b localization, NADPH oxidase assembly, and epithelial-mesenchymal transition. *Mol Biol Cell*. 2012; 23: 4097-4108.
 44. Sarbassov DD, Guertin DA, Ali SM, Sabatini DM. Phosphorylation and regulation of Akt/PKB by the rictor-mTOR complex. *Science* 2005; 307: 1098-1101.
 45. Yuan TL, Cantley LC. PI3K pathway alterations in cancer: variations on a theme. *Oncogene* 2008; 27: 5497-510.
 46. Ji H, Ding Z, Hawke D, Xing DM, Jiang BH, Mills GB, Lu ZM. AKT-dependent phosphorylation of Niban regulates nucleophosmin- and MDM2-mediated p53 stability and cell apoptosis. *EMBO Rep*. 2012; 13: 554-560.
 47. Mojsa B, Lassot I, Desagher S. Mcl-1 ubiquitination: unique regulation of an essential survival protein. *Cells* 2014; 3: 418-437.
 48. Porta C, Paglino C, Mosca A. Targeting PI3K/Akt/mTOR signaling in cancer. *Front Oncol*. 2014; 4: 64.
 49. Zhang J, Yu XH, Yan, YG, Wang C, Wang WJ. PI3K/Akt signaling in osteosarcoma. *Clinica Chimica Acta* 2015; 444: 182-192.
 50. Huang DW, Sherman BT, Lempicki RA. Systematic and integrative analysis of large gene lists using DAVID bioinformatics resources. *Nat Protoc*. 2009; 4: 44-57.
 51. Huang DW, Sherman BT, Lempicki RA. Bioinformatics enrichment tools: paths toward the comprehensive functional analysis of large gene lists. *Nucleic acids Res*. 2009; 37: 1-13.
 52. Wang Y, El-Zaru MR, Surks HK, Mendelsohn ME. Formin homology domain protein (FHOD1) is a cyclic GMP-dependent protein kinase I-binding protein and substrate in vascular smooth muscle cells. *J Biol Chem*. 2004; 279: 24420-24426.
 53. Wang Y, Zheng XR, Riddick N, Bryden M, Baur W, Zhang X, Surks HK. ROCK isoform regulation of myosin phosphatase and contractility in vascular smooth muscle cells. *Circ Res*. 2009; 104: 531-540.
 54. Goncalves V, Paulo Matos P, Jordan P. Antagonistic SR proteins regulate alternative splicing of tumor-related Rac1b downstream of the PI3-kinase and Wnt pathways. *Hu Mol Genet*. 2009; 18: 3696-3707.
 55. Gonçalves V, Henriques A, Pereira J, Costa AN, Moyer MP, Moita LF, Gama-Carvalho M, Matos P, Jordan P. Phosphorylation of SRSF1 by SRPK1 regulates alternative splicing of tumor-related Rac1b in colorectal cells. *RNA* 2014; 20: 474-482.
 56. Pulgar TGD, Bandrés E, Espina C, Valdés-Mora F, Pérez-Palacios R, García-Amigot F, García-Foncillas J, Lacal JC. Differential expression of Rac1 identifies its target genes and its contribution to progression of colorectal cancer. *Int. J. Biochem. & Cell Biol*. 2007; 39: 2289-2302.
 57. Clark GJ, Westwick JK, Der CJ. p120 GAP modulates Ras activation of Jun kinases and transformation. *J Biol Chem*. 1997; 272: 1677-1681.
 58. Visvikis O, Lore's P, Boyer L, Chardin P, Lemichez E, Gacon G. Activated Rac1, but not the tumorigenic variant Rac1b, is ubiquitinated on Lys 147 through a JNK-regulated process. *FEBS J*. 2008; 275: 386-396.